Intercepting the Disilene-Silylsilylene Equilibrium

COMMUNICATION

Intercepting the Disilene-Silylsilylene Equilibrium

Martin W. Stanford,[a] Julia I. Schweizer,[b] Maximilian Menche,[b] Gary S. Nichol,[a] Max C. Holthausen*[b] and Michael J. Cowley*[a]

Dedicated, with admiration, to Prof. Robert West on the occasion of his 90th birthday

Abstract: The equilibrium between disilenes ($R_2Si=SiR_2$) and their silylsilylene (R_3Si-SiR) isomers has previously been inferred but not directly observed, except in the case of the parent system $H_2Si=SiH_2$. Here, we report a new method to prepare base-coordinated disilenes with hydride substituents. By varying the bulk of the coordinating base and other silicon substituents, we have been able to control the rearrangement of disilene adducts to their silylsilylene tautomers. Remarkably, 1,2 migration of a trimethylsilyl group is preferred over hydrogen migration. A DFT study of the reaction mechanism provides a rationale for the observed reactivity and detailed information on the bonding situation in base-stabilized disilenes.

Disilene, Si_2H_4, is the silicon analogue of ethene. Unlike C_2H_4,[1] Si_2H_4 has several structural isomers (Scheme 1a) which lie close in energy according to quantum-chemical studies. Predictions of the relative energy of silylsilylene, $H_3Si–SiH$, place it between 5 – 10 kcal mol^{-1} above disilene, $H_2Si=SiH_2$.[2] In the chemical vapor deposition of silicon from silane, species such as $:SiH_2$, disilene, and silylsilylene are involved.[3] These low-coordinate intermediates are proposed to insert into Si–H bonds to form new Si–Si bonds.[4] Despite numerous theoretical studies on the disilene-silylsilylene equilibrium,[2a,5] experimental evidence is limited. In an argon matrix, silylsilylene interconverts with disilene upon photoirradiation.[5d] The same process has been inferred in the gas phase for the smallest organo-disilene, $Me_2Si=SiMe_2$ **I**. When generated by pyrolysis, tetramethyldisilene **I** is proposed to rearrange to its trimethylsilyl(methyl)silylene isomer **II** (Scheme 1b); this reactivity has also been observed for related disilenes.[6]

Persistent disilenes with bulky substituents have been widely studied, particularly in regard of the analogy to alkenes.[7] More recently, chemists have begun exploiting the differences between silicon and carbon chemistry, with the ability of disilenes to activate small molecules being revealed.[8] In contrast, isolable derivates of silylsilylenes are much less common, in line with the inherent lability caused by the strong σ-donating ability of silyl groups.[9]

Interconversion between isolable disilenes and silylsilylenes has not been directly observed, although this isomerization has been invoked several times to explain unanticipated reaction products or thermally induced rearrangements.[8b,10] For example, reduction of dibromosilane **III** (Scheme 1c) was proposed to result initially in silylsilylene **IV** which rearranged to the observed product, the disilene **V**.[10a] In the reverse direction, the rearrangement of disilene **VI** to **VIII** could only proceed by rearrangement to the silylsilylene **VII** followed by insertion into the Si–Cl bond (Scheme 1d).[10b] A related isomerization of cyclotrisilenes is induced by base-coordination.[11] Recently, a boryl-substituted disilene was reported to cleave two molecules of H_2; the proposed mechanism involves rearrangement of an intermediate disilene to a transient silylsilylene.[8b,c]

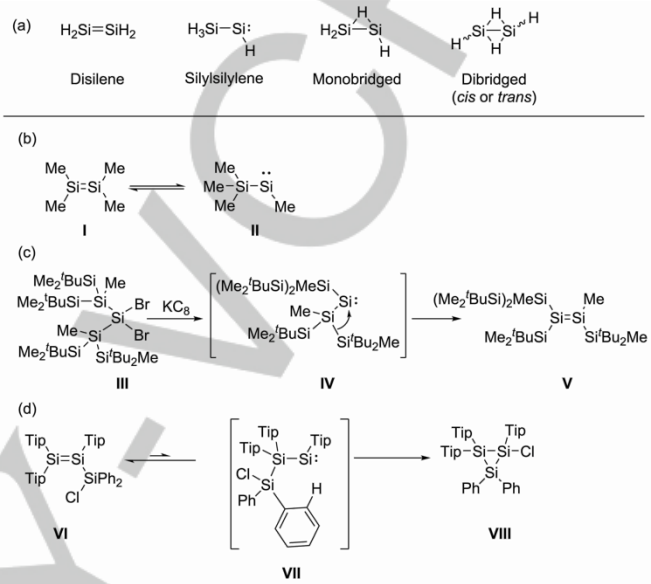

Scheme 1. (a) Isomers of Si_2H_4. (b-d) examples of proposed disilene-silylsilylene rearrangements.[6,10a,b] Tip = 2,4,6-tri*iso*propylphenyl.

Despite these many examples of the disilene to silylsilylene rearrangement, it has not yet been possible to directly observe this process in solution. Here, we show that by using a base-coordination strategy we can observe and control the isomerization of a disilene to a silylsilylene. Furthermore, we report a new and simple synthetic route towards disilenes with Si–H substituents.

Silanes **1** and **2** were prepared by treatment of Cp^*SiHCl_2[12] or Ar^*SiHCl_2[13] (Cp^* = pentamethylcyclopentadienyl, Ar^* = 2,6-bis(2,4,6-trimethylphenyl)phenyl) with the bulky silyl anion $(THF)_nKSi(SiMe_3)_3$.[14] Treatment of Cp*-substituted silane **1** with KO^{t}Bu in THF results in a complex mixture of products, as determined by ^{1}H NMR spectroscopy. However, when the same reaction is performed in the presence of the NHC 1,3-di*iso*propyl-4,5-dimethylimidazol-2-ylidene ($^{Me}I^iPr$), a clean transformation to the base-stabilized disilene **3** is observed. **3** was isolated as a

[a] Martin W. Stanford, Dr Gary S. Nichol, Dr. M. J. Cowley
School of Chemistry, University of Edinburgh
Joseph Black Building, David Brewster Road, Edinburgh, EH9 3FJ, UK.
E-mail: michael.cowley@ed.ac.uk

[b] Julia I. Schweizer, Maximilian Menche, Prof. Dr. Max C. Holthausen
Institut für Anorganische Chemie, Goethe-Universität
Max-von-Laue-Straße 7, 60438 Frankfurt/Main, Germany.
E-mail: max.holthausen@chemie.uni-frankfurt.de

Supporting information for this article is given via a link at the end of the document.

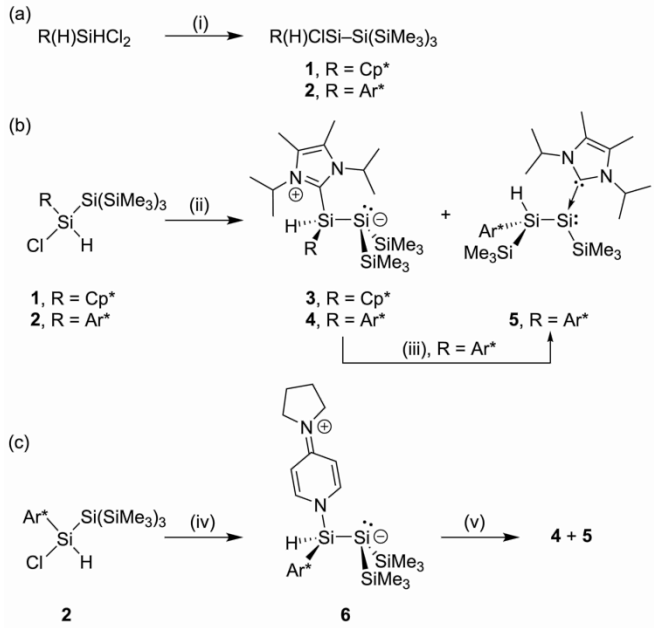

Scheme 2. Synthesis of compounds **1-6**. Cp* = pentamethylcyclopentadienyl, Ar* = 2,6-bis(2,4,6-trimethylphenyl)phenyl. Conditions and reagents: (i) $KSi(SiMe_3)_3(THF)_n$; (ii) KO^{t}Bu, ^{Me}I/^{i}Pr; (iii) 55 °C; (iv) KO^{t}Bu, 4-pyrrolidinopyridine; (v) ^{Me}I/^{i}Pr.

bright orange powder in 53% yield. In addition to an Si–H signal at δ 5.71 ($^1J_{H–Si}$ = 165 Hz), two septet signals at δ 5.83 and 5.06 are indicative of coordinated ^{Me}I/^{i}Pr,[15] which was confirmed by observation of the carbene carbon signal at δ 156.1 in the ^{13}C NMR spectrum. ^{29}Si NMR signals at δ −5.1, −13.0, and −202.2 ppm are assigned to the two $SiMe_3$ groups, the hydride-substituted silicon, and the three-coordinate $Si(SiMe_3)_2$ center, respectively. Together, the NMR data support the formulation of **3** as a base-coordinated disilene.

The solid-state structure of **3** was determined by single-crystal X-ray diffraction (Figure 1).[16] Although **3** can be considered a base-coordinated disilene, the long Si1–Si2 bond distance 2.3575(8) Å indicates the presence of a single bond. Moreover, Si2 is significantly pyramidalized (sum of bond angles = 296.15(5)°) signifying the presence of an electron lone pair and a formal negative charge at this center (cf. Lewis structure **3a** in Scheme 3). This is consistent with the high-field resonance observed for Si2 in the ^{29}Si NMR spectrum (δ −202.2), which is typical for silyl anions.[14,17] The NHC C1–Si1 bond distance, 1.945(2) Å, is typical of NHC-silicon bonds.[11b,18]

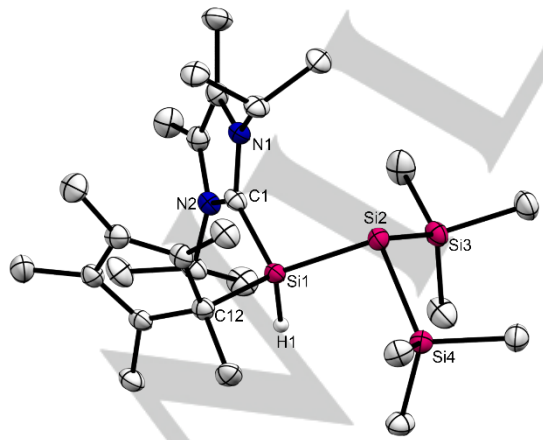

Figure 1. Solid state structure of disilene **3**. Hydrogen atoms, with the exception of H1, omitted for clarity. Thermal ellipsoids set to 50% probability. Selected bond lengths (Å) and angles (°): Si1-Si2 2.3575(8), Si1-C1 1.945(2), Si1-C12 1.947(2), Si2-Si3 2.3569(9), Si2-Si4 2.3611(8); Si1-Si2-Si4 94.97(3), Si3-Si2-Si1 101.61(3), Si3-Si2-Si4 99.57(3).

The NHC-coordinated disilene **3** is reminiscent of the amine-coordinated disilene $Me_2EtN{\rightarrow}SiCl_2{\rightarrow}Si(SiCl_3)_2$ **IX** recently reported by some of us (Scheme 3).[19] Scheme 3 shows the three major Lewis resonance representations of compound **3**: zwitterionic **3a**, disilene adduct **3b**, or with dative C–Si and Si–Si bonds (**3c**) as suggested for **IX**.[19] To evaluate the bonding in **3**, we performed density functional theory (DFT) calculations.[20] A Natural bond orbital (NBO) analysis reveals a natural localized molecular orbital (NLMO) with s-character representing the lone pair at Si2, whilst two further NLMOs correspond to 2e-2c Si1–Si2 and C1–Si1 single bonds, polarized towards Si1 and C1, respectively (Figure 2a). The NLMO corresponding to the C1–Si1 bond is notably less polarized than that for the amine N1–Si1 bond in **IX**[19] ([76%]C1–Si1[22%] vs. [86%]N1–Si1[12%]). Natural population analysis (NPA, Figure 2b) indicates a significant net-electron transfer from the carbene to Si1 in **3** (0.38 e), larger than that from the amine in **IX** (0.24 e). All characteristics for the Si1–Si2 interaction in **3** are essentially identical to those in **IX**.

Far reaching similarities between **3** and **IX** are also evident in the topological analysis of the computed electron density according to Bader's quantum theory of atoms in molecules (QTAIM).[21] QTAIM analysis of **3** discloses a molecular graph with bond paths between the central Si(H)Cp* group and the carbene C1 atom as well as the $Si(SiMe_3)_2$ fragment (see ESI). We interpret the topological characteristics of the 2D Laplacian shown in Figure 2c for the C1–Si1 and Si1–Si2 interactions as indicating dative bonding:[19,22] The bond critical points (bcp) are shifted towards the more electropositive bonding partner (Si1 and Si2, respectively) and reside close to nodal surfaces in the Laplacian distribution.[23] The 1D Laplacian profiles along the bond paths show a single pronounced VSCC minimum (valence-shell charge concentration) close to the more electronegative center and a mere shoulder for the other, both residing in the atomic basin of the donor (C1 and Si1, respectively). A central silylene fragment as part of a dative bond network C1→Si1→Si2 is also indicated by Haaland's definition of dative bonds (see ESI).[24] All in all, our bonding analyses reveal a very similar picture for the bonding situations in **3** and in **IX**, consistent with their structural parallels.

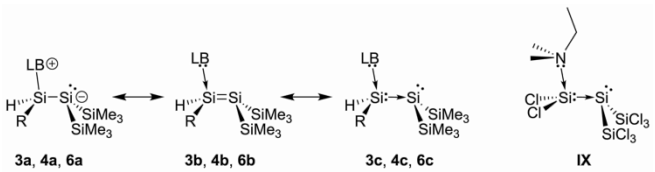

Scheme 3. Lewis structure representations of disilenes **3**, **4**, and **6** and **IX**.[19] **3**: R = pentamethylcyclopentadienyl, L = ^{Me}I/^{i}Pr. **4**: R = 2,6-bis(2,4,6-trimethylphenyl)phenyl, L = ^{Me}I/^{i}Pr. **6**: R = 2,6-bis(2,4,6-trimethylphenyl)phenyl, L = 4-pyrrollidinopyridine.

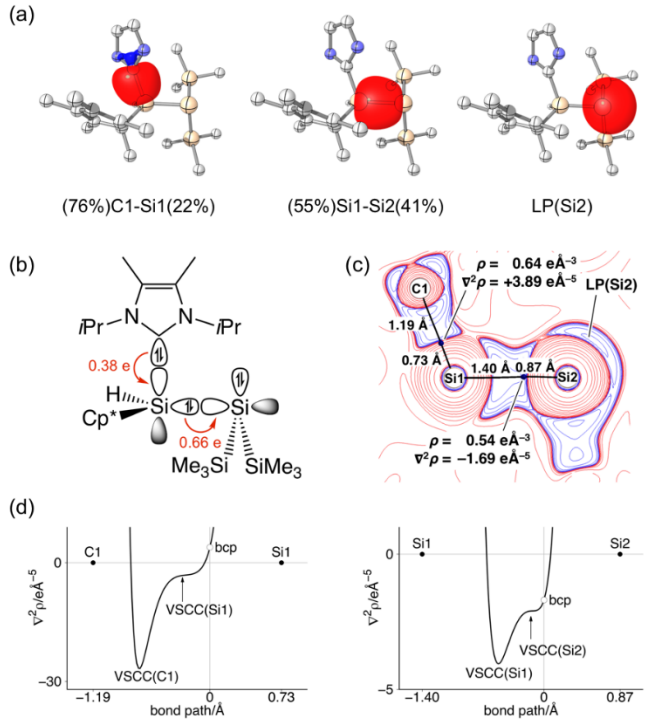

Figure 2. Bonding analysis of **3**. (a) NLMOs representing C1–Si1 and Si1–Si2 bonds and the lone pair at Si2. (b) Orbital interaction scheme with net electron transfer according to NPA. (c) 2D plot of $\nabla^2\rho(r)$; charge concentration (blue) and depletion (red), bond paths (black lines), and bcps (blue dots) with characteristic properties and distances. (d) 1D Laplacian profiles along C1–Si1 (left) and Si1–Si2 bond paths (right).

In contrast to the reaction of Cp*-substituted silane **1**, which leads to **3** as the sole observable product, treatment of the bulkier terphenyl-substituted **2** with KO^{t}Bu and ^{Me}I^{i}Pr delivers a mixture of two compounds. ^{1}H NMR spectroscopy reveals two new Si–H resonances at δ 5.49 ($^1J_{Si-H}$ = 178 Hz) and 3.91 ($^1J_{Si-H}$ = 155 Hz) in an approximate ratio of 1:1, as well as formation of Me$_3$SiO^{t}Bu. The signal at δ 5.49 is close in chemical shift to that observed for **3**. Furthermore, ^{1}H–^{29}Si correlation experiments revealed associated ^{29}Si signals at δ −4.8, −37.1 and −188.0, assigned to two SiMe$_3$, Si–H and Si(SiMe$_3$)$_2$ groups respectively. On the basis of the similarity with the spectrum of **3**, this species is identified as the NHC-coordinated disilene **4**. Heating the reaction mixture led to disappearance of **4**, whilst the Si–H signal at δ 3.91 grew in intensity. This latter compound, **5**, could be obtained preparatively in 41% yield by treatment of **2** with KOtBu and MeIiPr in THF at 60 °C.

The NHC-coordinated silylsilylene **5** has ^{29}Si NMR resonances at δ −11.8, −13.8, −69.8 and −121.4. The ^{29}Si signal at δ −69.8 is assigned to the Si–H group by ^{1}H–^{29}Si correlation experiments. The $^1J_{Si-H}$ coupling constant (155 Hz) and Si–H ^{1}H chemical shift (δ 3.91) are typical of four-coordinate silanes (e.g. $^1J_{Si-H}$ in HSi(SiMe$_3$)$_3$ = 156 Hz).[14] The two SiMe$_3$ groups are assigned to the signals at δ –11.8 and –13.8. The signal at δ –121.4 is found at higher field compared to other three-coordinate silylenes.[18a,25] ^{Me}I^{i}Pr coordination is confirmed by observation of the carbene carbon at δ 172.2 in the ^{13}C NMR spectrum.

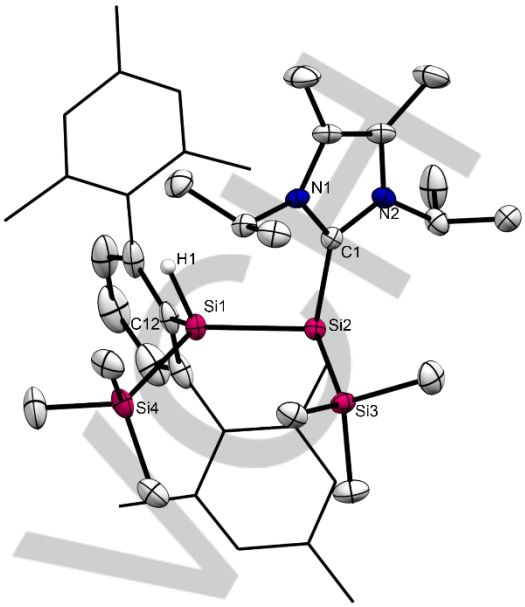

Figure 3. The solid-state structure of silylsilylene **5**. Hydrogen atoms except H1 omitted. Thermal ellipsoids at 50% probability. Selected bond lengths (Å) and angles (°). **5:** Si2-Si1 2.3674(9), Si2-Si3 2.3421(8), Si2-C1 1.960(2), Si1-Si4 2.3639(8); Si3-Si2-Si1 111.37(3), C1-Si2-Si1 102.35(7), C1-Si2-Si3 103.54(6).

The solid-state structure of the silylsilylene **5** is shown in Figure 3. The bond distance between the carbene and the three-coordinate silicon center is very similar to that of **3** (1.960(2) Å vs 1.945(2) Å). All Si–Si bond distances in **5** are within the expected range of single bonds (2.3421(8) – 2.3674(9) Å). The sum of angles at Si2 is 317.26° indicating the presence of an electron lone pair.

We attempted to obtain quantitative data about the conversion of NHC-coordinated disilene **4** to silylsilylene **5**. Monitoring the initially formed ~1:1 mixture by ^{1}H NMR in THF-d_8 (using mesitylene as an internal standard), we observed complete consumption of **4** within 3 hours at 55 °C ($t_{1/2}$ = 40 mins). Although all of the disilene adduct **4** is consumed, it is not converted quantitatively into **5**, indicating substantial decomposition of **4**. Reasoning that the initial step in the conversion is dissociation of the NHC ligand from **4**, and that the decomposition observed was exacerbated by high temperatures, we sought to prepare a more labile derivative of **4**.

Treatment of the terphenyl-substituted precursor **2** with KO^{t}Bu in the presence of 4-pyrollidinopyridine (4-PPy) afforded the fragile disilene adduct **6**, which decomposes in solution but can be isolated as a crude solid. The ^{29}Si chemical shift of the three-coordinate silicon center, at δ –184.0, is comparable to that of **3** and **4**. Replacement of the more strongly donating ^{Me}I^{i}Pr ligand of **3** with the weaker base 4-PPy results in the expected lower field chemical shift for the four-coordinate Si–H center of **6** (δ 34.7). The solid-state structure of **6**, crystallized in low yield, is shown in Figure S1. The structural features of **6** are broadly similar to those of **3**, though compared to **3** the shorter Si1–Si2 bond distance (2.3225(6) vs. 2.3575(8) Å) and less pyramidalised geometry at Si2 (sum of angles = 297.66(3)°) is consistent with the less basic 4-PPy ligand.

The 4-PPy ligand in **6** is labile and coordination appears reversible – the concentration of free PPy in d_8-THF solutions of **6** varies with temperature. In non-coordinating solvents (C_6D_6), **6** rapidly decomposes ($t_{½}$ ≈ 30 mins) with the release of 4-PPy at higher temperatures. The crude 4-PPy adduct **6** can be transformed into the silylsilylene **5** by exchange of the coordinating base. Thus, when excess $^{Me}I^{i}Pr$ is added to samples of **6**, the formation of **4** and **5** is observed by ^{1}H NMR spectroscopy.

Overall, the observation of **3**, **4**, **5**, and **6** under the same reaction conditions shows that the disilene/silylsilylene equilibrium can be controlled by the steric bulk of the coordinating base and the substituent. Further insight into the underlying isomerization mechanism is provided by DFT calculations (Scheme 4). The lowest-energy pathway from the terphenyl-substituted disilene adduct $\mathbf{A}^{Ar*}$ (cf. **4** above) commences with the endergonic NHC dissociation to form free disilene $\mathbf{B}^{Ar*}$ in a barrierless step. Alternative Si–Si bond cleavage to the silylene NHC adducts is kinetically strongly disfavored (Scheme S4, ESI). Isomerization of $\mathbf{B}^{Ar*}$ by silyl-migration via $\mathbf{TS}^{Ar*}$ leads to silylsilylene $\mathbf{C}^{Ar*}$, which is 4 kcal mol^{-1} less stable than disilene $\mathbf{B}^{Ar*}$, and NHC recoordination forms $\mathbf{D}^{Ar*}$ (cf. **5** above). Hydride migrations cannot compete kinetically (see ESI). Thus, the overall isomerization reaction is slightly exergonic with an activation barrier of 24 kcal mol^{-1}. $\mathbf{D}^{Ar*}$ can also be obtained starting from 4-PPy-coordinated disilene $\mathbf{E}^{Ar*}$ (cf. **6** above) through the same reaction cascade. As expected, 4-PPy is more weakly bound to the disilene moiety than the NHC, so that reaction of $\mathbf{E}^{Ar*}$ with (excess) NHC results in Lewis base exchange, yielding $\mathbf{A}^{Ar*}$ and eventually $\mathbf{D}^{Ar*}$. Analogous isomerization of the Cp*-substituted disilene adduct $\mathbf{A}^{Cp*}$ (cf. **3**) to the corresponding silylsilylene adduct $\mathbf{D}^{Cp*}$, however, is kinetically inhibited ($\Delta^{‡}G$ = 37 kcal mol^{-1}) and endergonic by 4 kcal mol^{-1}. The greater stability of the silylsilylene base-adduct $\mathbf{D}^{Ar}$ is a consequence of increased steric bulk in $\mathbf{A}^{Ar*}$.

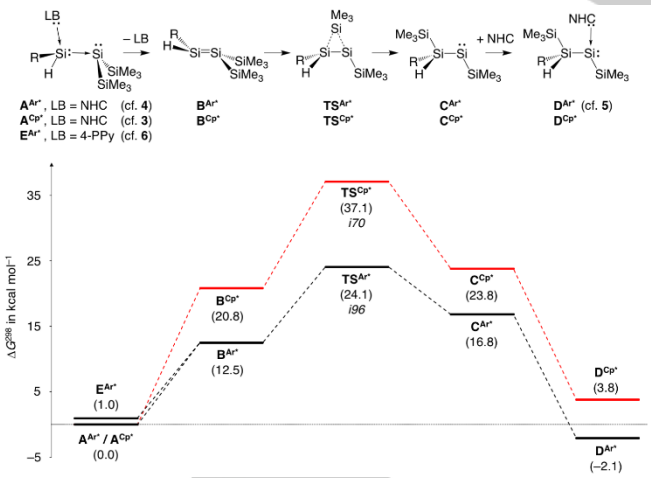

Scheme 4. Computed reaction profiles for the disilene/silylsilylene isomerizations (SMD-M06-2X/6-311++G(2d,2p)//RI-M06L/6-31+G(d,p), solvent THF; ΔG^{298} in kcal mol^{-1}). "*i70*" etc. denotes the imaginary frequency for the identified transition states. NHC = $^{Me}I^{i}Pr$ = 1,3-di*iso*propyl-4,5-dimethylimidazol-2-ylidene, 4-PPy = 4-pyrollidinopyridine; black profile: R = Ar* = 2,6-bis(2,4,6-trimethylphenyl)phenyl; red profile: R = Cp* = C_5Me_5.

In conclusion, we report a novel route for accessing base-stabilized low-valent silicon compounds, including a rare example of a silylsilylene. Direct observation of the disilene/silylsilylene equilibrium by NMR spectroscopy was possible, and structural characterization of compounds from both sides of equilibrium was also possible. Based on experimental and computational results, we propose a reaction mechanism involving an equilibrium between transient disilenes and silylsilylenes, and interception with Lewis bases.

Acknowledgements

MJC thanks the University of Edinburgh for a Chancellor's Fellowship. MWS thanks the Carnegie Trust for the award of a PhD Scholarship. Quantum-chemical calculations were performed at the Center for Scientific Computing (CSC) Frankfurt on the FUCHS and LOEWE-CSC high-performance compute clusters.

Keywords: silicon chemistry • low-coordinate• disilenes • silylenes • mechanism

[1] a) J. A. Pople, K. Raghavachari, M. J. Frisch, J. S. Binkley, P. V. R. Schleyer, *J. Am. Chem. Soc.* **1983**, *105*, 6389–6399; b) K. Raghavachari, M. J. Frisch, J. A. Pople, P. von R. Schleyer, *Chem. Phys. Lett.* **1982**, *85*, 145–149.

[2] a) G. Dolgonos, *Chem. Phys. Lett.* **2008**, *466*, 11–15; b) L. Sari, M. C. McCarthy, H. F. Schaefer, P. Thaddeus, *J. Am. Chem. Soc.* **2003**, *125*, 11409–11417; c) C. Pak, J. C. Rienstra-Kiracofe, H. F. Schaefer, *J. Phys. Chem. A* **2000**, *104*, 11232–11242; d) M. C. Ernst, A. F. Sax, J. Kalcher, *Chem. Phys. Lett.* **1993**, *216*, 189–193; e) L. A. Curtiss, K. Raghavachari, P. W. Deutsch, J. A. Pople, *J. Chem. Phys.* **1991**, *95*, 2433–2444; f) B. T. Luke, J. A. Pople, M. B. Krogh-Jespersen, Y. Apeloig, M. Karni, J. Chandrasekhar, P. v. R. Schleyer, *J. Am. Chem. Soc.* **1986**, *108*, 270–284; g) A. F. Sax, *J. Comput. Chem.* **1985**, *6*, 469–477; h) K. Krogh-Jespersen, *J. Phys. Chem.* **1982**, *86*, 1492–1495; i) R. A. Poirier, J. D. Goddard, *Chem. Phys. Lett.* **1981**, *80*, 37–41.

[3] *Ullmann's Encyclopedia of Industrial Chemistry*, Wiley-VCH, Weinheim, **2011**.

[4] F. Falk, G. Mollekopf, H. Stafast, *Appl Phys A* **1998**, *67*, 507–512.

[5] a) L. C. Snyder, Z. R. Wasserman, *J. Am. Chem. Soc.* **1979**, *101*, 5222–5223; b) H. Teramae, *J. Am. Chem. Soc.* **1987**, *109*, 4140–4142; c) H. Jacobsen, T. Ziegler, *J. Am. Chem. Soc.* **1994**, *116*, 3667–3679; d) G. Maier, H. P. Reisenauer, J. Glatthaar, *Chem. Eur. J.* **2002**, *8*, 4383–4391. e) S. Nagase, T. Kudo, *Organometallics* **1984**, *3*, 1320–1322.

[6] a) W. D. Wulff, W. F. Goure, T. J. Barton, *J. Am. Chem. Soc.* **1978**, *100*, 6236–6238. b) H. Sakurai, Y. Nakadira, H, Sakaba, *Organometallics* **1983**, *2*, 1484–1486.

[7] a) T. Iwamoto, S. Ishida, in *Functional Molecular Silicon Compounds II* (Ed.: D. Scheschkewitz), Springer International Publishing, **2013**, pp. 125–202; b) P. P. Power, *Nature* **2010**, *463*, 171–177; c) C. Präsang, D. Scheschkewitz, *Chem. Soc. Rev.* **2016**, *45*, 900–921; d) A. Rammo, D. Scheschkewitz, *Chem. Eur. J.* **2018**, *24*, 6866–6885.

[8] a) D. Wendel, T. Szilvási, C. Jandl, S. Inoue, B. Rieger, *J. Am. Chem. Soc.* **2017**, *139*, 9156–9159 b) T. Kosai, T. Iwamoto, *J. Am. Chem. Soc.* **2017**, *139*, 18146–18149; c) T. Kosai, T. Iwamoto, *Chem. Eur. J.* **2018**, *24*, 7774–7780.

[9] a) S.-H. Zhang, H.-X. Yeong, H.-W. Xi, K. H. Lim, C.-W. So, *Chem. Eur. J.* **2010**, *16*, 10250–10254; b) A. V. Protchenko, A. D. Schwarz, M. P. Blake, C. Jones, N. Kaltsoyannis, P. Mountford, S. Aldridge, *Angew. Chem. Int. Ed.* **2013**, *52*, 568–571; c) A. V. Protchenko, J. I. Bates, L. M.

A. Saleh, M. P. Blake, A. D. Schwarz, E. L. Kolychev, A. L. Thompson, C. Jones, P. Mountford, S. Aldridge, *J. Am. Chem. Soc.* **2016**, *138*, 4555–4564; d) A. Sekiguchi, T. Tanaka, M. Ichinohe, K. Akiyama, S. Tero-Kubota, *J. Am. Chem. Soc.* **2003**, *125*, 4962–4963.

[10] a) M. Ichinohe, R. Kinjo, A. Sekiguchi, *Organometallics* **2003**, *22*, 4621–4623; b) K. Abersfelder, D. Scheschkewitz, *J. Am. Chem. Soc.* **2008**, *130*, 4114–21; c) X.-Q. Xiao, H. Zhao, Z. Xu, G. Lai, X.-L. He, Z. Li, *Chem. Commun.* **2013**, *49*, 2706–2708; d) H. Kobayashi, T. Iwamoto, M. Kira, *J. Am. Chem. Soc.* **2005**, *127*, 15376–7; e) T. Sasamori, K. Hironaka, Y. Sugiyama, N. Takagi, S. Nagase, Y. Hosoi, Y. Furukawa, N. Tokitoh, *J. Am. Chem. Soc.* **2008**, *130*, 13856–13857; f) T. Agou, Y. Sugiyama, T. Sasamori, H. Sakai, Y. Furukawa, N. Takagi, J.-D. Guo, S. Nagase, D. Hashizume, N. Tokitoh, *J. Am. Chem. Soc.* **2012**, *134*, 4120–4123.

[11] a) K. Leszczyńska, K. Abersfelder, A. Mix, B. Neumann, H.-G. Stammler, M. J. Cowley, P. Jutzi, D. Scheschkewitz, *Angew. Chem. Int. Ed.* **2012**, *51*, 6785–8; b) M. J. Cowley, V. Huch, H. S. Rzepa, D. Scheschkewitz, *Nat. Chem.* **2013**, *5*, 876–879.

[12] A. H. Cowley, E. a. V. Ebsworth, S. K. Mehrotra, D. W. H. Rankin, M. D. Walkinshaw, *J. Chem. Soc., Chem. Commun.* **1982**, 1099–1100.

[13] C. Gerdes, W. Saak, D. Haase, T. Müller, *J. Am. Chem. Soc.* **2013**, *135*, 10353–10361.

[14] C. Marschner, *Eur. J. Inorg. Chem.* **1998**, *1998*, 221–226.

[15] a) H. Schneider, A. Hock, R. Bertermann, U. Radius, *Chem. Eur. J.* **2017**, *23*, 12387–12398; b) M. D. Francis, D. E. Hibbs, M. B. Hursthouse, C. Jones, N. A. Smithies, *J. Chem. Soc., Dalton Trans.* **1998**, 3249–3254; c) H. Braunschweig, W. C. Ewing, K. Geetharani, M. Schäfer, *Angew. Chem. Int. Ed.* **2015**, *54*, 1662–1665.

[16] CCDC 1859551 (**1**), 1859552 (**2**), 1859553 (**3**), 1859554 (**5**) and 1859555 (**6**) contain the supplementary crystallographic data for this paper. These data can be obtained free of charge from The Cambridge Crystallographic Data Centre.

[17] a) C. Marschner, *Organometallics* **2006**, *25*, 2110–2125; b) C. Präsang, D. Scheschkewitz, in *Functional Molecular Silicon Compounds II* (Ed.: D. Scheschkewitz), Springer International Publishing, **2013**, pp. 1–47.

[18] a) D. Lutters, C. Severin, M. Schmidtmann, T. Müller, *J. Am. Chem. Soc.* **2016**, *138*, 6061–6067; b) A. C. Filippou, O. Chernov, G. Schnakenburg, *Angew. Chem. Int. Ed.* **2009**, *48*, 5687–90; c) A. C. Filippou, Y. N. Lebedev, O. Chernov, M. Straßmann, G. Schnakenburg, *Angew. Chem. Int. Ed.* **2013**, *52*, 6974–6978; d) P. Ghana, M. I. Arz, U. Das, G. Schnakenburg, A. C. Filippou, *Angew. Chem. Int. Ed.* **2015**, *54*, 9980–9985; e) Y. Xiong, S. Yao, M. Driess, *J. Am. Chem. Soc.* **2009**, *131*, 7562–7563; f) R. S. Ghadwal, H. W. Roesky, S. Merkel, J. Henn, D. Stalke, *Angew. Chem. Int. Ed.* **2009**, *48*, 5683–6.

[19] J. I. Schweizer, M. G. Scheibel, M. Diefenbach, F. Neumeyer, C. Würtele, N. Kulminskaya, R. Linser, N. Auner, S. Schneider, M. C. Holthausen, *Angew. Chem. Int. Ed.* **2016**, *55*, 1782–1786.

[20] Geometry optimizations performed at the RI-M06-L/6-31+G(d,p) level; improved energies and wave functions were obtained from M06-2X/6-311++G(2d,2p) single-point calculations (with SMD model with THF as solvent for energies). See ESI.

[21] R. F. W. Bader, *Atoms in Molecules: A Quantum Theory*, Oxford University Press, Oxford, **1990**.

[22] a) P. Maachi, A. Sironi, in *The Quantum Theory of Atoms in Molecules (Eds.: C. F. Matta, R. J. Boyd)*, Wiley-VCH, Weinheim, **2007**; b) P. Macchi, A. Sironi, *Coordin. Chem. Rev.* **2003**, *238–239*, 383–412; c) R. S. Ghadwal, H. W. Roesky, S. Merkel, D. Stalke, *Chem. Eur. J.* **2010**, *16*, 85–88; d) P. L. A. Popelier, in *The Chemical Bond: Fundamental Aspects of Chemical Bonding (Eds.: G. Frenking, S. Shaik)*, Wiley-VCH, Weinheim, **2014**.

[23] The topological properties of the electron density at the bcp are commonly used for interpreting the nature of a bond:[22a] a high ρ(bcp) and negative $\nabla^2\rho$(bcp) indicate covalent bonding, while ionic closed-shell interactions exhibit a low ρ(bcp) and a positive $\nabla^2\rho$(bcp). For strongly polar-covalent bonding, however, the close proximity of bcps to nodal surfaces renders the sign of $\nabla^2\rho$(bcp) inconclusive. It is more instructive to interpret the 1D Laplacian profile along the bond path with respect to its shape and the position of minima (VSCC) along the graph.

[24] A. Haaland, *Angew. Chem. Int. Ed. Eng.* **1989**, *28*, 992–1007.

[25] a) S. Inoue, C. Eisenhut, *J. Am. Chem. Soc.* **2013**, *135*, 18315–18318; b) Y. Gao, J. Zhang, H. Hu, C. Cui, *Organometallics* **2010**, *29*, 3063–3065; c) R. Rodriguez, D. Gau, T. Kato, N. Saffon-Merceron, A. De Cózar, F. P. Cossío, A. Baceiredo, *Angew. Chem. Int. Ed.* **2011**, *50*, 10414–10416; d) R. Azhakar, R. S. Ghadwal, H. W. Roesky, H. Wolf, D. Stalke, *Organometallics* **2012**, *31*, 4588–4592.

Entry for the Table of Contents (Please choose one layout)

Layout 2:

COMMUNICATION

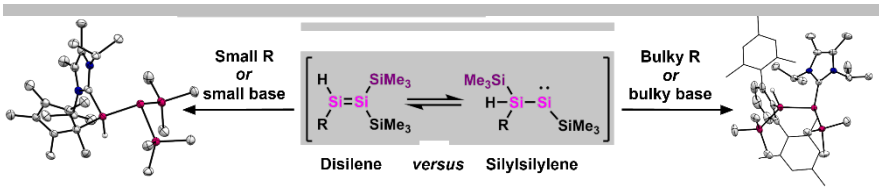

Martin W. Stanford, Julia I. Schweizer, Maximilian Menche, Gary S. Nichol, Max C. Holthausen and Michael J. Cowley**

Page No. – Page No.

Intercepting the Disilene-Silylsilylene Equilibrium

The isomerization of disilene, Si_2H_4, to its silylsilylene tautomer occurs readily. Stable disilenes with bulky substituents display reactivity that indicates the same rearrangement can occur, but experimental observations of the silylsilylene isomers are rare. We report base coordinated hydridodisilenes that rearrange to their silylsilylene isomers, together with a detailed mechanistic study of the transformation.